Numerical analysis of Huygens-like on-chip antennas for mm-wave applications

Numerical analysis of Huygens-like on-chip antennas for mm-wave applications

Dmitrii Kruglov, Marianna Ivashina, Oleg Iupikov, Rob Maaskant
Department of Electrical Engineering, Chalmers, Gothenburg, Sweden, dmitrii.kruglov@chalmers.se

***Abstract*—As we transition to 5G and beyond, the frequencies increase and the efficiency of the antennas becomes a pressing issue. Silicon technologies are preferred when it comes to en masse user equipment production, but the antennas in silicon suffer from high dielectric losses and strong substrate waves coupling. The use of a Huygens source as the antenna element has a potential of decreasing these negative effects, as was demonstrated in several non-silicon PCB designs. In this paper, we investigate if a similar performance enhancement can be achieved in thin back-gated silicon antenna chips. We present a numerical comparison of an electric dipole, a magnetic dipole and a Huygens source antenna at 120 GHz on a lossy silicon substrate sitting on a ground plane. Antennas are defined in MATLAB as distributed currents and imported as near-field sources into CST Microwave Studio. This way we treat the problem in a very general way without regards for any particular physical antenna implementations. Radiation efficiency and gain are shown as functions of substrate thickness. We found that there is no apparent advantage of using a Huygens source over either electric or a magnetic dipole in the described setup. We argue that this result is based on the fact that the Huygens source is derived assuming infinite current sheets at the interface of two infinite homogeneous regions, and propose another definition for a Huygens source in multi-layer structures.**

***Index Terms*—on-chip-antennas, mm-wave antennas, Huygens source, EM simulations.**

I. Introduction

To satisfy the ever-growing demand for broader bandwidths and higher data rates, researchers are now interested in designing antennas for millimeter-wave frequencies that would be power-efficient, cost-effective and easy to scale in large arrays. Silicon is the preferred material when it comes to mass production and high level of integration. At high frequencies, however, silicon is a very lossy material, which severely limits the radiation efficiency of on-chip-antennas (AoC) [1]. However, the state-of-the-art solutions in silicon of the last couple of years demonstrate radiation efficiencies as high as 50–60% [2], and it is now becoming feasible to consider the AoC approach over the ultimately better performing, but more costly, antenna-in-package (AiP) solutions.

A popular choice of a radiating element is an electric dipole. It is well understood, easy to fabricate and to interface with the active circuitry. For example, a state-of-the-art silicon AoC from [3] operates in the 138–151 GHz frequency range, has a high radiation efficiency (62%) and demonstrates high Equivalent Isotropica Radiated Power (EIRP, 11 dBm). To minimize the losses in silicon, a thin 100 µm substrate was chosen, two dipoles were used to cancel the substrate waves and a ground plane acts as a reflector to redirect the back-radiated fields. One hypothetical way to further decrease the radiation into the substrate, which is the leading source of losses, is to use the Huygens source as a radiator.

A Huygens source is a theoretical point source consisting of a point electric and an orthogonal point magnetic dipole that are scaled such as to cancel the back-radiation (in the far field). When placed at the interface between air and silicon, the electric dipole will mostly radiate into silicon ($\approx 97\%$ of the power), whereas the magnetic dipole and Huygens source radiate more then 75% and 90% into air correspondingly [4]. Although this is true for an interface between two infinite homogeneous regions, the question remains whether the situation is similar for thin grounded substrates that are commonly used in silicon production. A ground plane significantly improves the dipole gain due to the fact that all power is radiated away from the ground. However, due to the high permittivity of silicon, strong surface wave coupling may occur [5], lowering the amount of power available for radiation in the desired direction. Granted, the near-field of a Huygens source is not as directive as its far-field, but it is to be investigated whether there is potentially less power being transferred into the substrate waves.

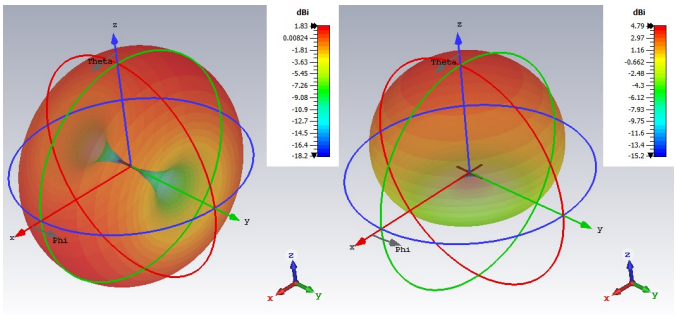

Fig. 1. Simulated radiation patterns of an electric or a magnetic dipole (left) and of a Huygens current source in free space (right).

Various antenna designs with Huygens-like radiation patterns were successfully fabricated and measured, using different approaches to Huygens source realization: e.g. coupling an electric dipole to a current loop [6], using helical antennas [7], using metamaterial-inspired solutions [8] and others. More importantly, several designs of electrically small Huygens antennas in planar multilayered geometries have recently been demonstrated, showing the potential of these types of devices

for AoC applications. In [6] the authors stacked two high-performance laminate substrates containing magnetic and electric dipole elements coupled to a feed. This approach leads to an endfire radiation pattern and a more compact vertical size of the device in comparison to the broadside radiating schemes where one the dipoles must be placed perpendicular to the substrate. The simulated directivity of the proposed antenna is 4.66 dBi and is close to the theoretical limit 4.77 dBi, and the simulated radiation efficiency is above 60%. Even though the device operates at a relatively low frequency (≈1GHz) and it is not a mass-production process, it shows that it is in principle possible to build a planar Huygens antenna. Another great example is a planar antenna for 5G at 28 GHz [9] where the emphasize was put on the scalability. High radiation efficiency of $\approx 80\%$ and high gain of almost 4 dBi was demonstrated. None of the described designs use a ground plane.

In this paper, we compared the radiation performance of an electric and a magnetic dipole with that of a Huygens-like antenna on silicon chip. In Sec. I we provided the motivation for this study and a literature review of some state-of-the-art solutions. In Sec. II we describe how we define antenna as distributed current sources, what is the simulation setup and parameters, and what are the assumptions that we made in our analysis. For the sake of generality, we compared the idealized distributed current sources rather than actual antenna implementations. Then, in Sec. III we show radiation efficiency and gain simulation results for an electric dipole, a magnetic dipole and a Huygens source. In Sec. IV we discuss our findings. Finally, we provide a short conclusion of our work in Sec. V.

II. Problem Setup

A. Defining the sources

In practice, Huygens antenna designs have complicated structures. Our goal is to compare dipole antennas, both electric and magnetic, and a Huygens source performances on a chip with the least possible assumptions about the antenna geometry. For that, we treat the former as distributed electric or distributed magnetic currents, and the latter as a distributed electric and an orthogonal magnetic currents. We define a current source in MATLAB, then calculate the E- and H- near fields on the surface of a box enclosing the source and import these fields into CST [10] as a near-field source.

In a homogeneous medium, the radiated E- and H-fields from an electric and magnetic surface current $\boldsymbol{J}$ and $\boldsymbol{M}$ are found, respectively, as (c.f. [11]):

$$\boldsymbol{E}_J = \eta C_k \iint_{S'} [\boldsymbol{J} C_{N_1} - (\boldsymbol{J}\cdot\hat{\boldsymbol{R}})C_{N_2}]\frac{e^{-jkR}}{R}dS' \tag{1a}$$

$$\boldsymbol{H}_J = -C_k \iint_{S'} (\boldsymbol{J}\times\hat{\boldsymbol{R}})C_N \frac{e^{-jkR}}{R}dS' \tag{1b}$$

$$\boldsymbol{E}_M = C_k \iint_{S'} (\boldsymbol{M}\times\hat{\boldsymbol{R}})C_N \frac{e^{-jkR}}{R}dS' \tag{1c}$$

$$\boldsymbol{H}_M = \frac{1}{\eta}C_k \iint_{S'} [\boldsymbol{M} C_{N_1} - (\boldsymbol{M}\cdot\hat{\boldsymbol{R}})C_{N_2}]\frac{e^{-jkR}}{R}dS', \tag{1d}$$

where k is the wavenumber in the medium, $\eta = \sqrt{\mu/\epsilon}$ is the wave impedance, and $C_k = -jk/(4\pi)$, $C_{N_1} = 1+\frac{1}{jkR}-\frac{1}{(kR)^2}$ and $C_{N_2} = 1+\frac{3}{jkR}-\frac{3}{(kR)^2}$. In the following analysis we will assume a y-aligned distributed electric dipole current of length L and width W centered around the origin. The surface current distribution is approximated as

$$\boldsymbol{J}(x,y) = J_0 \sin[k(L/2-|y|)]\hat{\boldsymbol{y}}, \tag{2}$$

with $|y| < L/2$ and $|x| < W/2$, and zero elsewhere. J_0 is the current amplitude. Similarly, we will assume an equally-sized orthogonal equivalent magnetic dipole current,

$$\boldsymbol{M}(x,y) = M_0 \sin[k(L/2-|x|)](-\hat{\boldsymbol{x}}). \tag{3}$$

Next, the continuous surface currents are expanded into a discrete set of sub-sectional pulse-shaped basis function currents, i.e.,

$$\boldsymbol{J} = \sum_{n=1}^{N} J_n \Pi_n(\boldsymbol{r})\hat{\boldsymbol{y}} \quad \text{and} \quad \boldsymbol{M} = \sum_{m=1}^{M} M_m \Pi_m(\boldsymbol{r})\hat{\boldsymbol{x}} \tag{4}$$

where $\{J_n\}_{n=1}^{N}$ and $\{M_m\}_{m=1}^{M}$ are the corresponding sets of expansion coefficients for the currents. The pulse function $\Pi_n(\boldsymbol{r}) = 1$ in cell S_n and zero elsewhere.

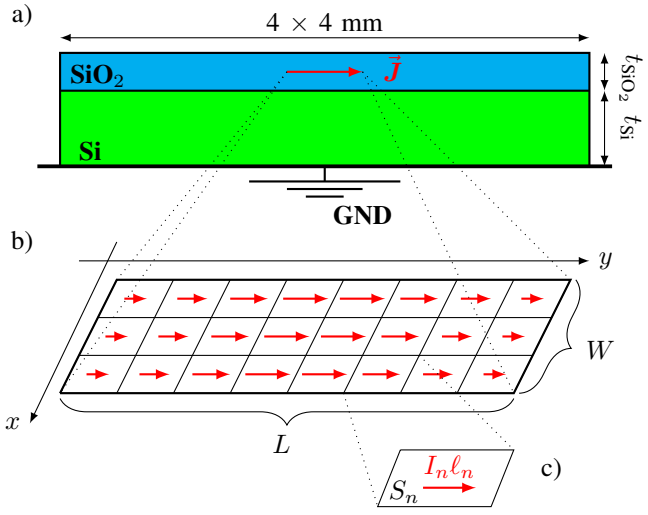

Fig. 2. Chip geometry (a). An electric current source is broken into n cells S_n (b), each cell having its area A_n and a dipole moment $I_n\ell_n$ (c). An analogous procedure is carried out for a magnetic dipole $\boldsymbol{M}$.

Substituting (4) in (1) and using the midpoint integration

rule, the fields are computed numerically as

$$\boldsymbol{E}_J = \eta C_k \sum_{n=1}^{N} J_n A_n [C_{N_1} - \hat{\boldsymbol{R}}_{y,n} C_{N_2}] \frac{e^{-jkR_n}}{R_n} \tag{5a}$$

$$\boldsymbol{H}_J = -C_k \sum_{n=1}^{N} J_n A_n (\hat{\boldsymbol{y}} \times \hat{\boldsymbol{R}}_y) C_N \frac{e^{-jkR_n}}{R_n} \tag{5b}$$

$$\boldsymbol{E}_M = C_k \sum_{m=1}^{M} M_m A_m (\hat{\boldsymbol{x}} \times \hat{\boldsymbol{R}}_m) C_N \frac{e^{-jkR_m}}{R_m} \tag{5c}$$

$$\boldsymbol{H}_M = \frac{1}{\eta} \sum_{m=1}^{M} M_m A_m [C_{N_1} - \hat{\boldsymbol{R}}_{x,m} C_{N_2}] \frac{e^{-jkR_m}}{R_m}, \tag{5d}$$

where A_n is the area of cell n, $R_n = |\boldsymbol{r} - \boldsymbol{r}_n|$ is the distance from the observation point $\boldsymbol{r}$ to the geometrical center (midpoint/centroid) $\boldsymbol{r}_n$ of the cell S_n. The corresponding unit vector $\hat{\boldsymbol{R}}_n$ points from this centroid to the observation point. The coefficient J_n is known since this represents the sample of the current in the midpoint of cell S_n, see Fig. 2(b). Note that, since J_n is in A/m, $J_n A_n = I_n \ell_n$ is in A·m and $I_n \ell_n$, which is known as the electric dipole moment of cell S_n.

Likewise we also sum the fields of equivalent magnetic dipole moments. The mainstream time-domain 3D EM-solvers do not have the functionality to define impressed magnetic currents excitation, thus the novelty of this approach.

B. Geometry and simulation parameters

The finite-element time-domain (FDTD) solver in CST Studio Suite was used for the EM analysis. Simulations were carried out in a simplified chip structure shown in Fig. 2(a). The electric dipole antenna is defined as a $\hat{y}$-oriented electric current source in the middle of a $14\,\mu\text{m}$-thick lossless silicon dioxide layer which is stacked on top of the lossy silicon substrate (with varied thickness). The magnetic dipole antenna is defined analogously as a $(-\hat{x})$-oriented magnetic current source. The Huygens source is defined as a $\hat{y}$-oriented electric and an orthogonal $(-\hat{x})$-oriented magnetic source pair scaled as $|\boldsymbol{M}| = \eta_0 |\boldsymbol{J}|$. Both dipoles are 220 µm long ($\approx 0.1\lambda_0$). The whole structure is placed on an infinite ground plane. The permittivity of SiO_2 is $\epsilon_r = 4.1$, and for Si is $\epsilon_r = 11.9$. Silicon conductivity is taken $\sigma = 2$ S/m.

The back-end-of-line (BEoL) metallization was omitted to speed up the simulations. In practice, there are several metal layers present, and strict metal density rules have to be satisfied. For that, dummy metal fillings are often patterned into and around the antenna layer, which leads to antenna performance degradation (c.f. for example [12]). However, it was shown that there are ways to reduce this effect to a minimum, e.g. the fills configuration number 8 from [13] introduces almost no reduction in the gain of the antenna when the fills are small enough.

Antennas are often patterned in the top metal layer just microns from the air interface, but in our model we placed it deeper into the dioxide layer so that the imported field sources are fully submerged in the dielectric. The SiO_2 layer is assumed lossless, and its thickness is much smaller than that of the silicon layer, therefore the placement of a source does not affect the generality of the problem.

We expect an electric dipole placed on a grounded silicon substrate to radiate maximum power at about 0.07 λ_0 substrate thickness [14]. To maximize the gain of a dipole antenna at this point, the size of the chip needs to be larger than the free-space wavelength λ_0 and to be an odd number of the silicon's half-wavelengths $\lambda_{Si}/2$ to minimize the re-radiation along the surface of the chip due to the substrate waves. In our case, we found that at 120 GHz the gain is maximised at chip size of 4×4 mm. These were chosen and kept constant during simulations for all sources.

III. Simulation results

Fig. 3 shows the simulation results for the radiation efficiency

$$\eta_{\text{rad}} = P_{\text{rad}} / (P_{\text{rad}} + P_{\text{loss}}) \tag{6}$$

at 120 GHz as a function of the silicon thickness. P_{rad} is the total radiated power, and P_{loss} is the power dissipated in silicon (the ground plane is assumed lossless). For very small substrate thicknesses the electric dipole (blue curve) gets shortened and almost does not radiate any power. The maximum efficiency $\approx 60\%$ occurs at the substrate thickness around 0.06–0.07 λ_0 which is in a good agreement with the theoretical results for a dipole on a grounded dielectric substrate (described e.g. in [14]). At $h \approx 0.2\lambda_0$ a minimum in substrate waves power is predicted [14], and this is where we see the second efficiency peak $\approx 38\%$. The radiation efficiency of a magnetic dipole (green curve) reaches 100% as the Si thickness approaches zero because we assume a lossless ground plane in our simulations. In practical designs that use magnetic dipoles (slot antennas), the efficiency often is well beyond 50% for very small substrate thicknesses due to metal losses (for example, in [15]). Then up until $\approx 0.2\lambda_0$ the magnetic dipole has a higher radiation efficiency than the electric dipole. Two reasons for that are that the silicon substrate is non-magnetic ($\mu = \mu_0$) and that the image of a magnetic dipole doesn't change sign. Substrate-waves coupling is of the same order of magnitude as for the electric dipole [14]. The radiation efficiency of the Huyngens source lies in-between the curves for the electric and the magnetic dipole.

Gain G_0 was calculated as the product of directivity D_0 in the broad-side direction and the radiation efficiency η_{rad}

$$G_0[\text{dBi}] = D_0[\text{dBi}] + \eta_{rad}[\text{dB}]. \tag{7}$$

We see from Fig. 4 that the curve representing the Huygens source gain (red curve) lies mostly between the corresponding curves for an electric (blue) and a magnetic (green) dipole. Exceptions are the small range of substrate thicknesses 0.12–0.15 λ_0 where the Huygens source's gain is higher than that of the electric/magnetic dipole, and two regions 0.07–0.08 λ_0 and 0.26–0.30 λ_0 when it is actually lower. When looking at the gain peaks at 0.07, 0.09 and 0.17 λ_0 it does not seem that using Huygens source would provide any advantage over

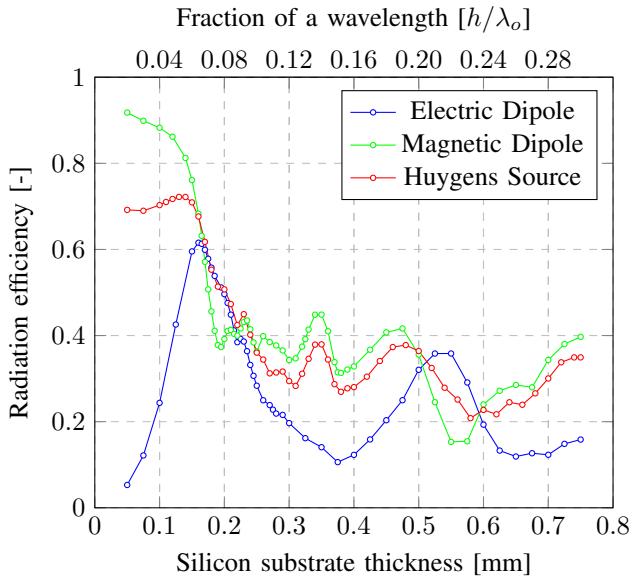

Fig. 3. Radiation efficiency as a function of silicon substrate thickness for the electric dipole (blue), magnetic dipole (green) and Huygens source (red) near field sources. Note that the ohmic losses are not included.

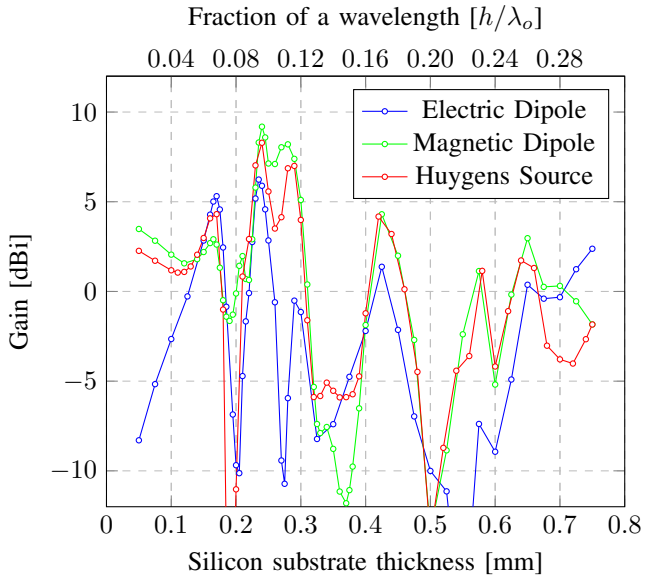

Fig. 4. Gain as a function of silicon substrate thickness for the electric dipole (blue), magnetic dipole (green) and Huygens source (red) near field sources.

electric/magnetic dipole. Constructive inference between the sources, their images and the re-radiation from the substrate waves at these three points results in high directivity ($>$ 10dBi) in the broadside direction and thus in high gain even though the radiation efficiency is low ($\leq$ 60%).

IV. Discussion

The result of over 90% Huygens source into-the-air radiation from [4] is the solution for the infinite current sheets on the border of two infinite homogeneous dielectrics. In this model, the Green's functions inside those dielectrics are of the form

$$\boldsymbol{G} \propto \frac{e^{-k_z|z-z_0|}}{2jk_z}. \tag{8}$$

Based on that, one can find a closed-form expression for $P_{\text{rad, air}}/P_{\text{rad, dielectric}}$ and find that to maximize this ratio the electric and the magnetic current sheets must be scaled as

$$|\boldsymbol{M}| = \eta|\boldsymbol{J}|. \tag{9}$$

In a grounded multi-layer structure, however, the Green's functions inside the substrate are very different from (8), and then (9) is no longer an appropriate condition for maximizing the into-the-air radiation. We suggest calculating the Green's functions for the electric and for the magnetic current sources in such structures (e.g. by spectral-domain methods [16]), taking the scaling and the mutual orientation of the currents as parameters. Such arrangement of the magnetic and an electric currents that maximize $P_{\text{rad, air}}/P_{\text{rad, dielectric}}$ for a particular multi-layer geometry can then be called a *multi-layer Huygens source*.

Another consequence of (8) is that the substrate waves are not present in the solution. It is known that these modes have a drastic negative effect on the radiation performance [17] and introduce heavy dependence on the chip sizes [18], especially for higher-permittivity dielectrics like silicon [5]. We see from our simulations (Fig. 3) that for an electric dipole there is only 60% of power radiated into air at best, mainly due to the substrate wave (SW) coupling [14]. Antenna engineers try to reduce the effect of SW by micro-machining cavities under the radiating elements [19], shielding off the high-permittivity substrates [15], using artificial electromagnetic band-gap (EBG) structures [20], etc. All those techniques make the chip structure very complex, and the performance of an antenna then depends on the particular design.

V. Conclusion

In this work we studied radiation performance of an electric dipole, a magnetic dipole and their combination known as the Huygens source. Numerical analysis was performed for the case of a back-grounded silicon substrate with dimensions and properties resembling commercially available solutions. We found that using a Huygens source will not improve the antenna gain when compared to either an electric or a magnetic dipole. We also discussed the issues with the Huygens source definition that lead to this result.

Acknowledgment

This work has received funding from the European Union's Horizon 2020 research and innovation programme under the Marie Skłodowska-Curie grant agreement No 860023 (for the contributions by D. Kruglov). Furthermore, the in-kind contribution by R. Maaskant, O. Iupikov, and M. Ivashina to this work has been supported by ChaseOn Centre in Integrated Antenna Array project financed by Vinnova, Chalmers University of Technology, Royal Institute of Technology (Stockholm), Ericsson, Saab, Ruag Space, Keysight, and Gapwaves.

References

[1] H. M. Cheema and A. Shamim, "The last barrier: On-chip antennas," *IEEE Microwave Magazine*, vol. 14, no. 1, pp. 79–91, 2013.

[2] R. Karim, A. Iftikhar, B. Ijaz, and I. B. Mabrouk, "The potentials, challenges, and future directions of on-chip-antennas for emerging wireless applications—a comprehensive survey," *IEEE Access*, vol. 7, pp. 173 897–173 934, 2019.

[3] A. Visweswaran, K. Vaesen, S. Sinha, I. Ocket, M. Glassee, C. Desset, A. Bourdoux, and P. Wambacq, "A 145GHz FMCW-radar transceiver in 28nm CMOS," in *2019 IEEE International Solid-State Circuits Conference-(ISSCC)*, IEEE, 2019, pp. 168–170.

[4] R. W. Ziolkowski, "Custom-designed electrically small huygens dipole antennas achieve efficient, directive emissions into air when mounted on a high permittivity block," *IEEE Access*, vol. 7, pp. 163 365–163 383, 2019.

[5] D. M. Pozar, *Microwave engineering, copyright 2012 by john wiley & sons*.

[6] S.-H. Lee, G. Shin, S. M. Radha, J.-Y. Choi, and I.-J. Yoon, "Low-profile, electrically small planar huygens source antenna with an endfire radiation characteristic," *IEEE Antennas and Wireless Propagation Letters*, vol. 18, no. 3, pp. 412–416, 2019.

[7] C. Morlaas, B. Souny, and A. Chabory, "Helical-ring antenna for hemispherical radiation in circular polarization," *IEEE Transactions on Antennas and Propagation*, vol. 63, no. 11, pp. 4693–4701, 2015.

[8] R. W. Ziolkowski, P. Jin, and C.-C. Lin, "Metamaterial-inspired engineering of antennas," *Proceedings of the IEEE*, vol. 99, no. 10, pp. 1720–1731, 2010.

[9] M.-C. Tang, T. Shi, and R. W. Ziolkowski, "A study of 28 GHz, planar, multilayered, electrically small, broadside radiating, huygens source antennas," *IEEE Transactions on Antennas and Propagation*, vol. 65, no. 12, pp. 6345–6354, 2017.

[10] (Oct. 2020). "CST Studio Suite," [Online]. Available: https : / / www . 3ds . com / products - services / simulia / products/cst-studio-suite.

[11] P.-S. Kildal, *Foundations of antenna engineering: a unified approach for line-of-sight and multipath*. Artech House, 2015.

[12] M. K. Hedayati, A. Abdipour, R. S. Shirazi, M. J. Ammann, M. John, C. Cetintepe, and R. B. Staszewski, "Challenges in on-chip antenna design and integration with rf receiver front-end circuitry in nanoscale CMOS for 5g communication systems," *IEEE Access*, vol. 7, pp. 43 190–43 204, 2019.

[13] X. Guo, R. Li, *et al.*, "Design guidelines for reducing the impact of metal interference structures on the performance on-chip antennas," in *IEEE Antennas and Propagation Society International Symposium. Digest. Held in conjunction with: USNC/CNC/URSI North American Radio Sci. Meeting (Cat. No. 03CH37450)*, IEEE, vol. 1, 2003, pp. 606–609.

[14] D. B. Rutledge, D. P. Neikirk, and D. P. Kasilingam, "Integrated circuit antennas," *Infrared and millimeter waves*, vol. 10, no. 2, pp. 1–90, 1983.

[15] S. Pan and F. Capolino, "Design of a CMOS on-chip slot antenna with extremely flat cavity at 140 GHz," *IEEE Antennas and Wireless Propagation Letters*, vol. 10, pp. 827–830, 2011.

[16] Z. Sipus, P.-S. Kildal, R. Leijon, and M. Johansson, "An algorithm for calculating green's functions of planar, circular cylindrical, and spherical multilayer substrates," *Applied Computational Electromagnetics Society Journal*, vol. 13, pp. 243–254, 1998.

[17] A. Babakhani, X. Guan, A. Komijani, A. Natarajan, and A. Hajimiri, "A 77-GHz phased-array transceiver with on-chip antennas in silicon: Receiver and antennas," *IEEE Journal of Solid-State Circuits*, vol. 41, no. 12, pp. 2795–2806, 2006.

[18] U. Johannsen, A. Smolders, R. Mahmoudi, and J. Akkermans, "Substrate loss reduction in antenna-on-chip design," in *2009 IEEE Antennas and Propagation Society International Symposium*, IEEE, 2009, pp. 1–4.

[19] R. Wang, Y. Sun, M. Kaynak, S. Beer, J. Borngräber, and J. C. Scheytt, "A micromachined double-dipole antenna for 122–140 GHz applications based on a SiGe BiCMOS technology," in *2012 IEEE/MTT-S International Microwave Symposium Digest*, IEEE, 2012, pp. 1–3.

[20] P. Kaul, A. Aljarosha, A. B. Smolders, P. Baltus, M. Matters-Kammerer, and R. Maaskant, "An E-band silicon-IC-to-waveguide contactless transition incorporating a low-loss spatial power combiner," in *2018 Asia-Pacific Microwave Conference (APMC)*, IEEE, 2018, pp. 1528–1530.